Thong Duc Hong
Ho Chi Minh City University of Technology (HCMUT)
Vietnam National University Ho Chi Minh City (VNU-HCM)
Vietnam

Minh Quang Pham
Ho Chi Minh City University of Technology (HCMUT)
Vietnam National University Ho Chi Minh City (VNU-HCM)
Vietnam

Phong Giang
Ho Chi Minh City University of Technology (HCMUT)
Vietnam National University Ho Chi Minh City (VNU-HCM)
Vietnam

Phat Tan Truong
Ho Chi Minh City University of Technology (HCMUT)
Vietnam National University Ho Chi Minh City (VNU-HCM)
Vietnam

Huong Huu Nguyen
Nguyen Tat Thanh University
Vietnam

Study on Designing a Diesel Firefighting Pump System for Residential Building

Currently, on-site diesel firefighting pump systems are significantly necessary for high-rise buildings. This study presents a process for designing diesel fire pump systems for high-rise buildings using AVL BOOST software associated with mechanical calculations. The Kirloskar CPHM 80/32 pump and DESSUN 4DSP-75 diesel engine were selected based on preliminary calculations to match the requirements of Vietnamese standards for a 79-meter building. AVL BOOST software has been used to simulate the full load performance characteristic of the engine; then, a partial load characteristic is determined for the adequate pump that requires input power at a rated speed of about 2975 rpm. The transmission consists of the propeller drive, and flanges were designed to connect the engine and pump. The findings show that utilizing AVL BOOST software is considerably helpful in determining the engine's partial load characteristics, saving time and costs. This study contributes a foundation for practical research to calculate and design the firefighting pump mechanical systems in high-rise buildings.

Keywords: *diesel engine, firefighting pump, performance characteristics, AVL BOOST, propeller shaft.*

1. INTRODUCTION

In the context of the service economy developing rapidly, the population in cities is sharply increasing. It leads to residential areas with more high-rise buildings being built to accommodate this increase. With high population density, ensuring fire safety in these buil–dings is vital [1]. Particularly, higher floors are often out of the reach of firefighters for high-rise buildings with a height of 120 meters or higher [2,3]. As a result, on-site fire pump systems are necessary for high-rise buildings. Fire pumps are essential equipment for pumping water from local water supplies to the top areas of high-rise buildings and even to the nozzles of each room's fire suppression system. The design and installation of fire pumps must be carefully calculated to ensure fire protection standards; otherwise, the fire protection system may not operate properly, leading to loss of property or even life in case of fire [4,5].

Fire pump systems in high-rise buildings normally consist of a main fire pump (usually an electric pump), a backup fire pump (usually a diesel or gasoline engine pump), and a pressure compensation pump [6]. The system can operate automatically via an electric pump when a fire or explosion occurs. However, if there is a break in the electricity supply, the system must be operated manually with the diesel pump. That is why diesel engine fire pump systems are always equipped in high-rise buildings. Besides, diesel engines are more often used in fixed firefighting systems than gasoline engines due to their high capacity, low speed, long lifespan, and lower maintenance than gasoline engines [7].

Diesel engine fire pump systems usually include a fire pump, a diesel engine, and a coupling between the diesel engine and the pump. Fire pumps are usually rotary dynamics pumps and are selected based on floor area, building height, the density of firefighting equip–ment, and the required pressure [7]. From there, engi–neers can choose a diesel engine with the appropriate capacity and rotational speed to drive the pump. The diesel engine and pump are linked together through transmissions such as belt drive, couplings, or propeller shafts, depending on the working conditions and design requirements of the system.

A crucial aspect of a fire pump system is the matching between the diesel engine and the fire pump. The diesel engine must have a larger capacity than the water pump; however, it must be manageable to diminish operating costs. Previously, when designing a building firefighting system, the engine's required power was often calculated based on the pump's maxi–mum capacity. Then, the engine was selected based on the engine's full load characteristics (i.e., maximum power). But in reality, diesel engines should operate at a power that is lower than the maximum power to ensure longevity and stability [8,9]. Therefore, choosing the engine and operating mode becomes difficult. Engineers must choose a considerable factor of safety (e.g., 1.5) to ensure system performance. Suppose it is possible to determine the partial-load characteristics of an internal combustion engine. In that case, it will be beneficial to select the engine and the appropriate operating mode accurately. AVL BOOST software will simulate the

Received: December 2023, Accepted: February 2024
Correspondence to: Dr. Thong Duc Hong, Ho Chi Minh City University of Technology, Ly Thuong Kiet Street 268, District 10, Ho Chi Minh City, Vietnam
E-mail: hongducthong@hcmut.edu.vn
doi: 10.5937/fme2402196T

engine's characteristics under different load modes, offering enterprises more options [10-12]. However, the number of publications on engine partial-load characteristics simulation is limited [13-15]. There was a great deal of relevant study on simulating engines; however, there is still a smaller amount on simulating engines driving firefighting water pumps.

Besides, choosing and calculating suitable drives for diesel engines and fire pumps is also important. Belt or chain drives achieve flexibility on transmission ratios but require periodic maintenance and are bulky in size. Couplings or propeller shafts provide compact structures and high stability, but the transmission ratio is limited to 1 [16]. Depending on the type of engine selected for the firefighting system, the drive type is determined to harmonize these factors.

In this study, the authors designed a diesel engine fire pump system to serve a 79-meter-tall building with 22 floors and 321 apartments. Firstly, the Kirloskar CPHM 80/32 pump and DESSUN 4DSP-75 diesel engine were selected based on preliminary calculations to match the capacity and speed of the firefighting system according to Vietnamese standards, as presented in Section 2. Secondly, AVL BOOST software is used to determine the appropriate operating mode for the engine and pump, as presented in Section 3. Finally, a propeller drive between the engine and pump is calculated and designed to comply with the working conditions and design requirements presented in Section 4. This work aims to contribute a practical method for designing diesel fire pump systems that are effective in both technical and economic terms.

2. INITIAL CALCULATIONS

Figure 1 presents the schematic diagram of the diesel firefighting pump system. The system consists of a centrifugal water pump with output power, P_{p_out}, efficiency, η_p, and required input power, P_{p_in}; a diesel engine with an output power of P_e; and transmission with transmission ratio, i_{tr}, and efficiency, η_{tr}. The engine drives the water pump via the transmission, so the engine output power is declined due to the efficiency of the transmission and pump.

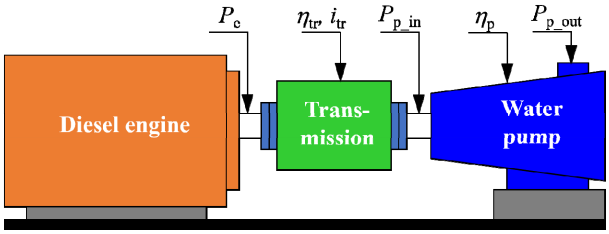

Figure 1. Diesel firefighting pump principle diagram.

According to current standards in Vietnam on fire protection systems, a 79-meter building with 22 floors building needs a firefighting pump system with a flow rate of 121.6 m^3/h and a pressure head of 128.2 m. Based on that, the Kirloskar CPHM 80/32 pump, with the ability to produce a rated flow rate of 122 m^3/h and head of 130m at a speed of 2975 rpm [17], was selected to suit the above building. Pump efficiency $\eta_p = 0.6586$. The pump characteristics are shown in Figure 2. These characteristics are built based on the similarity rules of commercial centrifugal pumps with the manufacturer's parameters [18]. The influence of viscosity is ignored. Pump efficiency is assumed to be constant. The pump characteristics are calculated as follows [18]:

Pump output power at rated speed, $P_{p\_out\_rate}$:

$$P_{p\_out\_rated} = \rho g H_{rated} Q_{rated} \quad (1)$$

where ρ is the fluid density, g is gravity acceleration, $H_{rated,}$ and Q_{rated} is the head and flow rate of a pump at rated speed.

Required input power of pump at rated speed, $P_{p\_in\_rate}$:

$$P_{p\_in\_rated} = P_{out\_rated} / \eta_p \quad (2)$$

Flow rate of pump, Q:

$$Q = Q_{rated} \left(n / n_{rated} \right) \quad (3)$$

where n is the pump speed

Head of pump, H:

$$H = H_{rated} \left(n^2 / n_{rated}^2 \right) \quad (4)$$

Required input power of pump, P_{p_in}:

$$P_{p\_in} = P_{p\_in\_rated} \left(n^3 / n_{rated}^3 \right) \quad (5)$$

Required input torque of pump, $T_{p\_in\_rate}$:

$$T_{p\_in} = P_{p\_in} / n \quad (6)$$

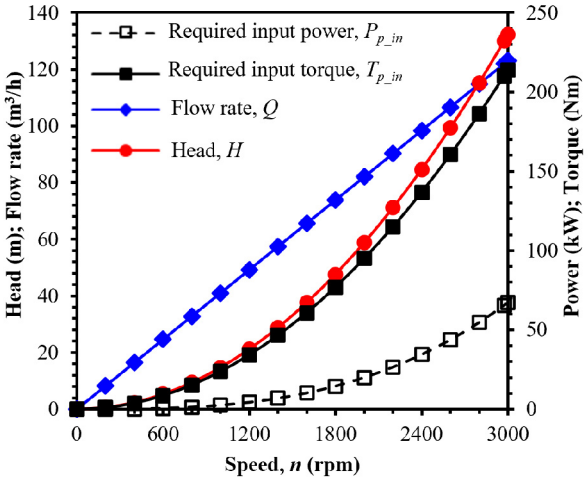

Figure 2. Kirloskar CPHM 80/32 pump characteristics

As indicated in Figure 2, at the rated speed of 2975 rpm, the maximum required input power P_{p_in} is 65.48 kW. Choosing the transmission efficiency η_{tr} of 0.95. The power of the engine driving pump can be calculated using the following equation [16]:

$$P_e = P_{p\_in} / \eta_{tr} = 65.48/0.95 = 68.92 \text{ (kW)} \quad (7)$$

In consequence, the engine must generate a power greater than 68.92 kW to ensure the pump can operate. Because it is not allowable for engines to run at 100% load with maximum power, the engine should be run at a lower 90% maximum power [8]. The diesel engine of

DESSUN 4DSP-75 with a maximum power of 75 kW at 3000 rpm was selected to ensure this requirement. The engine specification data [19] are shown in Table 1.

Table 1. Common specifications of the proposed engine [19]

Engine code	4DSP-75
Engine type	I4 stroke, direct injection, water cooling, turbocharger
Bore×Stroke	108×118 mm
Compression ratio	17.5:1
Maximum power	75 kW at 3000 rpm
Maximum torque	296 Nm at 2000 rpm
Dry weight(kg)	342
Dimension (L×W×H)	985×545×961mm

3. SIMULATING THE ENGINE PERFORMANCE CHARACTERISTICS AND DETERMINING THE WORKING CONDITION

3.1 Simulation model

Figure 3 illustrates the simulation model's primary components of the DESSUN 4DSP-75 diesel engine, including the engine, cylinder, and plenum, as well as the restriction elements, pipes, and system boundary, which are established in AVL BOOST environments [20]. In a four-cylinder turbo-charged diesel engine model, measuring points (MP) are used to measure gas conditions and flow information across a crank angle at a specific pipe site. The simulation model consists of two system boundaries (SB), where the first system boundary (SB1) is connected to the turbocharger (TC1), the plenum (PL1), and four pipes 4, 5, 8, and 9 representing the intake manifold. The exhaust manifolds (pipes 6, 7, 11, and 12) are connected to two plenums (PL2 and PL3) and the turbocharger (TC1) through two exhaust pipes 2 and 10. Finally, pipe 13 and the second system boundary (SB2) represent the engine's exhaust pipe.

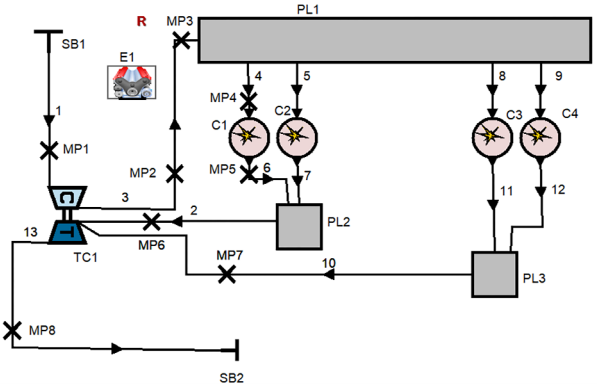

Figure 3. Four cylinders turbo-charged diesel engine AVL BOOST simulation model

3.2 Simulation process

Figure 4 shows the simulation process using AVL BOOST for the current study. AVL BOOST simulation models are built based on the proposed engine specifications. The experimental torque, power, and fuel consumption rate of the DESSUN 4DSP-75 engine were supplied by the manufacturer [19] at full load (100% engine load). The real fuel consumption rate was used as an input parameter for the simulation process. The indicated mean effective pressure ($IMEP_{sim}$), friction mean effective pressure ($FMEP_{sim}$), and brake mean effective pressure ($BMEP_{sim}$) were computed in the simulation.

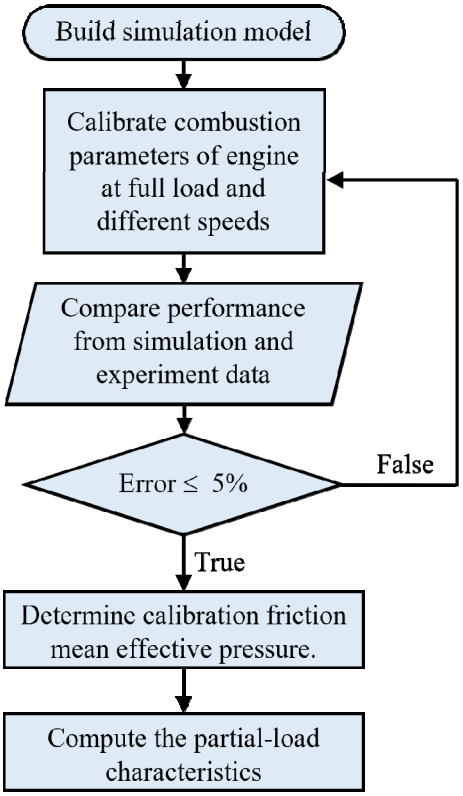

Figure 4. Simulation process using determining partial engine load characteristics

Then, simulation torque (T_{sim}) and power (P_{sim}) were determined by the equations as [21]:

$$T_{sim} = \frac{BMEP_{sim} V_D}{4\pi} \tag{8}$$

where V_D displacement volume

$$P_{sim} = 2\pi n T_{sim} \tag{9}$$

The power and torque characteristics obtained from simulation results were compared to those experiment data. The relevant parameters, such as combustion duration, combustion ignition, air-fuel ratio, engine operation temperature, etc., were varied in the AVL BOOST simulation model until the errors were archived at less than 5%.

After that, the calibration friction mean effective pressure ($FMEP_{cal}$) was calculated so that the torque and power obtained from the simulation were the same as those of experimental values by the following expressions [21]:

$$FMEP_{cal} = IMEP_{sim} - BMEP_{exp} \tag{10}$$

where $BMEP_{exp}$ is the experiment brake mean effective pressure, which is determined as [21]:

$$BMEP_{exp} = \frac{4\pi T_{exp}}{V_D} \tag{11}$$

where T_{exp} is the experimental torque

The $FMEP_{cal}$ was used to compute the partial engine loads. The performance characteristics of the engine at partial loads are obtained by varying the fuel cons–umption rate percentages corresponding to the expected engine loads.

3.3 Determining the working conditions of the engine

Figure 5 shows the engine characteristics at 91% and 100% load in tandem with the pump's required input power and torque. The AVL simulation process obtai–ned the characteristic curves at 91% and 100% load. Additionally, pump characteristics are determined based on the manufacturer's parameters. First of all, it is evidently seen that the power and torque of the engine at 100% load are significantly higher than those of the pump at all operating speeds, which means it is nece-ssary to determine a characteristic at a lower engine load to comply with the requirements of the water pump. Therefore, the engine load is gradually reduced until the engine's torque and the power curves at the pump input shaft intersect the pump's required input power and torque curve at the pump's rated speed of 2975 rpm. Since the maximum speed of the pump and the engine are approximately equal, the transmission ratio i_{tr} is chosen to be 1. Finally, it can be clearly seen that when the engine load is adjusted to 91%, the engine characteristic curves at the pump input shaft intersect the corresponding curves of the pump at a speed of 2975 rpm. As a result, the characteristic at 91% is the most suitable operating mode for the engine. The cha–racteristics achieved by AVL software guarantee that the diesel engine certainly drives the water pump in all cases.

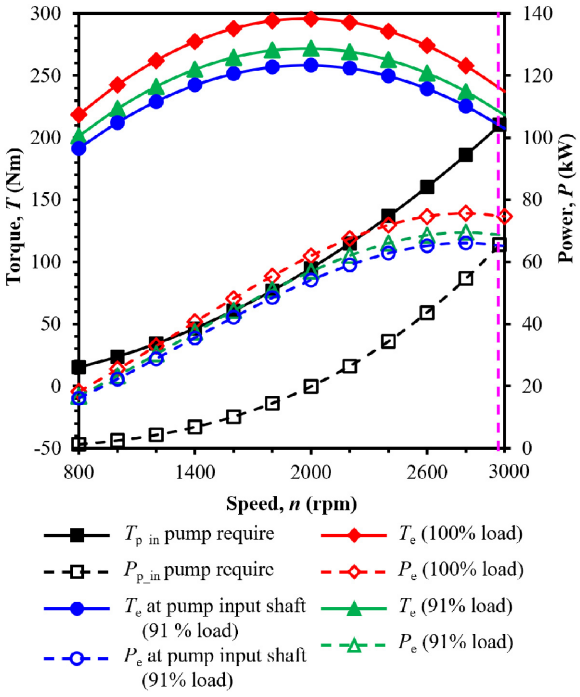

Figure 5. Power and torque characteristic curves of the engine and water pump

4. DESIGNING THE TRANSMISSION SYSTEM

According to the selected i_{tr} = 1, the propeller drive is chosen for the system because of its compact structure and flexibility. Figure 6 illustrates the exploded view of the propeller drive. The propeller shaft is the main component that either links or transmits the power from the engine to the water pump. The propeller shaft cluster includes 2 companion flanges, 2 flange yokes, a propeller shaft, and a universal cross joint. The companion flange I is connected between the flywheel and the end of the flange yoke by a group of bolts. Meanwhile, the companion flange II is used to connect the other end flange yoke and the water pump shaft with a group of bolts and a square key. All these components are taken into account in this section by considering the dimensions and strength.

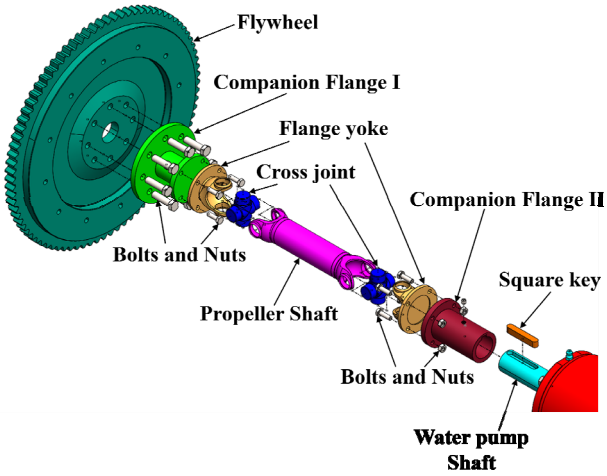

Figure 6. Exploded view of propeller drive

JIS G3101 SS400 Steel [22] is assumed to be used for all components' calculating processes, and the factor of safety ($F.S$) is chosen at 3. In this calculation, the compressive and tensile yield strength is supposed to be equal, which is $S_{yt} = S_{yc} = 400$ MPa [17].

Allowable compressive and shear stresses, when taking into account the factor of safety ($F.S$), are determined as below [17]:

$$[\sigma] = \frac{S_{yc}}{F.S} = \frac{S_{yt}}{F.S} = 133.33 \text{ (MPa)} \tag{12}$$

where $[\sigma]$ is the allowable compressive stress (MPa), $F.S$ = 3 is the factor of safety. S_{yt} and S_{yc} are the yield strength in tension and compression, respectively.

Based on the maximum shear stress theory of fai–lure, the shear yield strength is half of the tensile yield strength [17]. Hence, the following formula is used to calculate the allowable shear stress [17]:

$$[\tau] = \frac{0.5S_{yt}}{F.S} = 66.66 \text{ (MPa)} \tag{13}$$

where $[\tau]$ is the allowable shear stress (MPa) since the engine produces 296 Nm of maximum torque at 2000 rpm. Hence, the preliminary selection of the Gewes size 30 KZ 47 propeller shaft without length compensation in tandem with the corresponding size flanges yoke and cross joint.

The parameters of the Gewes KZ 47 propeller shaft without length compensation are summarized in Figure 7 and Table 2 below [23]:

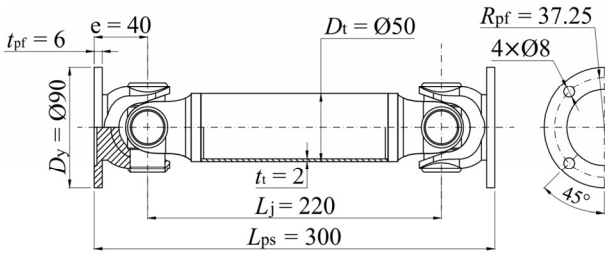

Figure 7. Drawing of Gewes KZ 47 propeller shaft

Table 2. Parameter of Gewes KZ 47 propeller shaft [23]

Parameter	Symbol	Value	Unit
Size	*KZ*	47	-
Length between joints center	L_j	220	mm
Overall length	L_{ps}	300	mm
Center of U-joint bore to end of the flange yoke	e	40	mm
Outer diameter and thickness of the propeller tube	$D_t \times t_t$	50 × 2	mm
Outer diameter of the flange yoke	D_y	90	mm
flange yoke pitch circle radius of bolts	R_{pf}	37.25	mm
Thickness of the propeller's flange	t_{pf}	6	mm

3.4 Calculating propeller shaft strength

Critical bending speed of propeller shaft

The critical bending speed of the propeller shaft is the speed at which the rotating shaft becomes dynamically unstable and starts to vibrate violently in a transverse direction [23-25]. According to the general layout design, the initial overall length of propeller shaft L_{ps} is selected at 300 mm. Hence, the distance between joints center L_j is 220 mm. Thus, for the propeller shaft, assuming the connection components have adequate flexural rigidity, the critical bending speed can be calculated using the following formula [23]:

$$n_{cri} = 0.9\times10^8 \times \frac{\sqrt{{D_t}^2 + {d_t}^2}}{L^2} = 126336.85 \text{ (rpm)} \quad (14)$$

where n_{cri} is the critical bending speed of the propeller shaft (rpm), D_t = 50 mm and d_t = 46 mm are the outer and inner diameter of the propeller tube shaft, and L = 220 mm is the distance between the joints center.

Maximum shear stress of propeller shaft

The polar modulus of propeller shaft tube section is calculated as follows [26]:

$$Z_t = \frac{\pi}{16D}\left({D_t}^4 - {d_t}^4\right) = 6960.76 \text{ (mm}^3\text{)} \quad (15)$$

where Z_t is the polar modulus of propeller shaft tube section (mm^3)

The maximum shear stress of the propeller shaft tube is determined by the following formula [27]:

$$\tau_{t.max} = \frac{T\times10^3}{Z_t} = 42.52 \text{ (MPa)} \quad (16)$$

where $\tau_{t.max}$ is the maximum shear stress of the propeller tube shaft (MPa), and T = 296 Nm is the maximum torque of the engine.

At 2000 rpm, the maximum torque T of the engine is 296 Nm, creating the maximum shear stress $\tau_{t.max}$ = 42.52 MPa < [τ] = 66.66 MPa. Hence, the propeller shaft ensures the strength condition of the system.

Strength of circular fillet weld subjected to torsion of propeller shaft

The size of the welded joint is calculated by the following formula [27]:

$$s = \frac{2.83\times T\times10^3}{\pi\tau_{weld}\times {D_t}^2} = 1.33 \text{ (mm)} \quad (17)$$

where s is the size of the weld (mm), τ_{weld} = 80 (MPa) is the maximum stress for the welded joint [27].

Hence, we select the size of the weld joint as s = 3 (mm) to comply with the recommended minimum size of welds [27].

3.5 Calculating cross joint

In order to have a constant rotational speed of the engine and the water pump, the propeller shaft is equipped with a universal cross joint at each end. The diameter of the cross joint's pins, therefore, is determined by the following formula [27]:

$$d_{cp} = \sqrt{\frac{T\times10^3}{2\times\frac{\pi}{4}\times[\tau]\times D_t}} \geq 7.52 \text{ (mm)} \quad (18)$$

where d_{cp} is the diameter of the cross pin (mm), [τ] = 66.66 MPa is the allowable shear stress for the pin (According to the allowable shear stress of JIS G3101 SS400 steel in section 4.).

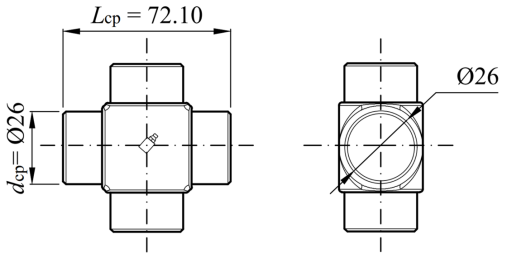

Figure 8. Drawing of Gewes size 30 cross joint

The cross joint's pin diameter must be at least 7.72 mm. Hence, the selected Gewes size 30 cross joint, the geometric parameters of which are shown in Figure 8, ensures the condition of the calculation above.

3.6 Designing of companion flange coupling

Two companion flange couplings are not only mounted on the propeller shaft ends in order to connect the engine and water pump but are also used to transmit the

torque from the engine to the water pump. Thus, the design and safety conditions are taken into account below.

Designing of companion flange I connecting water pump shaft with the yoke

Figure 9 shows the design and geometric parameters of companion flange I. The companion flange I is designed to connect the water pump shaft with the propeller shaft via M8 socket set screw cup point, one square key, and a set of bolts. The design, calculation, and safety verification of it are presented below.

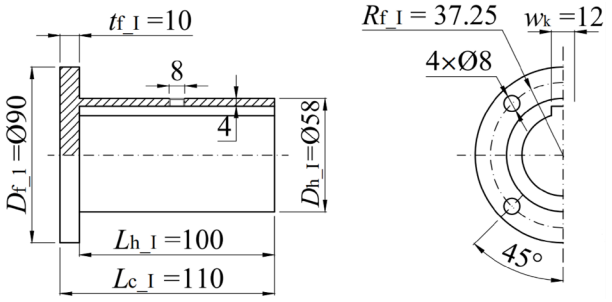

Figure 9. Drawing of companion flange I

Designing for the hub of the companion flange I

The outer diameter of hub D_{h_I} is preliminarily designed at 58 mm, and the inner diameter of the hub is equal to the diameter of the water pump shaft ($d_{h\_I} = d_p = 42$ mm).

The length of hub L_{h_I} is determined to be 100 mm in order to comply with the length of the water pump shaft.

The polar modulus of the hub section is calculated as follows [26]:

$$Z_{h\_I} = \frac{\pi}{16 D_{h\_I}} \left({D_{h\_I}}^4 - {d_{h\_I}}^4 \right) = 27776.01 \text{ (mm}^3\text{)} \quad (19)$$

where Z_{h_I} is the polar modulus of the companion flange's hub section (mm^3), D_{h_I} = 58 mm is the outer diameter of the hub.

Checking the induced shear stress for the hub material by the following formula [27]:

$$\tau_{h\_I} = \frac{T \times 10^3}{Z_{h\_I}} = 10.66 \text{ (MPa)} \quad (20)$$

where τ_{h_I} is the shear stress of the hub (MPa).

Since the shear stress of the hub is less than [τ]. Thus, the design of the hub is safe.

Designing for the flange of companion flange I

The thickness of flange t_{f_I} is preliminary designed at 10 mm

The flange at the junction of the hub is under shear while transmitting the torque. Hence, the shear stress in the flange is checked by the following formula [27]:

$$\tau_{f\_I} = \frac{T \times 10^3}{\frac{\pi {D_{h\_I}}^2}{2} \times t_{f\_I}} = 5.60 \text{ (MPa)} \quad (21)$$

where τ_{f_I} is the shear stress in flange (MPa).

Since the shear stress in the flange is less than the allowable shear stress value of the material, the design of the flange ensures strength.

The outer diameter of flange D_{f_I} is designed to comply with the outer diameter of the flange yoke, which has a value of 90 mm.

Designing for bolts of companion flange I

Due to the water pump shaft's diameter d_p is 42 mm. The number of companion flange I's bolts z_{bI}, therefore, is selected at 4 [27]. Thus, the companion flange's pitch circle radius of bolts R_{b_I} = 37.25 is taken to be equal to that of the flange yoke. The bolts are made of steel material with the allowable shear and crushing stress of its are [τ_b] = 50 MPa and [σ_{cb}] = 100 MPa [27], respectively.

The bolts are subjected to shear stress due to the torque transmitted. Hence, the nominal diameter of bolts is determined as follows [27]:

$$d_{b\_I} = \sqrt{\frac{T \times 10^3}{\frac{\pi R_{b\_I}}{4} \times [\tau_b] \times z_{b\_I}}} = 7.14 \text{ (mm)} \quad (22)$$

where d_{b_I} is the nominal diameter of the bolt (mm), R_{b_I} = 37 mm is the companion flange's pitch circle radius of bolts, [τ_b] = 50 MPa [27], and z_{b_I} = 4 is the number of bolts.

Hence, selecting the nearest standard size of the bolt is M8, which is the same as the flange yoke's nominal diameter of the bolt.

The bolts withstand shear stress due to the torque transmitted. Thus, the maximum shear stress on the bolts is determined as below [27]:

$$\tau_{b\_I.max} = \sqrt{\frac{T \times 10^3}{\frac{\pi R_{b\_I}}{4} \times d_{b\_I} \times z_{b\_I}}} = 17.78 \text{ (MPa)} \quad (23)$$

where $\tau_{b\_I.max}$ is the maximum shear stress on the bolts (MPa).

Since the maximum shear stress on the bolts is smaller than the allowable shear stress of bolt [τ_b] = 50 MPa. Hence, the bolts ensure the operating condition of the system.

Then, the maximum crushing stress of all the bolts is verified as follows [27]:

$$\sigma_{cb\_I.max} = \frac{T \times 10^3}{R_{b\_I} \times z_{b\_I} \times d_{b\_I} \times t_{f\_I}} = 24.83 \text{ (MPa)} \quad (24)$$

where σ_{cb_I} is the maximum crushing stress of bolts (MPa), *and* t_{f_I} = 10 mm is the thickness of the flange.

From the equation above, the induced crushing stress in the bolts is less than the allowable value of 100 MPa. Therefore, the design of the bolts is safe.

Designing the key of the companion flange I

The key is designed with the usual proportions and then verified for shearing and crushing stresses. Moreover, to simplify the manufacturing and assembling process, the length of the key is equal to the length of the hub, which is $L_k = L_{h\_I}$ =100 mm.

Since the crushing stress for the key material is two times higher than its shearing stress [26], the square key type is selected to be used. From [18], with the water pump's shaft diameter d_p is 42 mm and the width of the water pump's key is 12 mm, the thickness (t_k) and width (w_k) of key correspondence are equal, which have the value of 12 mm.

Considering the key withstands maximum shearing stress by the following formula [27]:

$$\tau_{k.max} = \frac{T \times 10^3}{L_k \times w_k \times \frac{d_{h\_I}}{2}} = 11.75 \text{ (MPa)} \quad (25)$$

where $\tau_{k.max}$ is the maximum shearing stress of the square key (MPa), w_k =12 mm, and L_k = 100 mm are the width and length of the key, respectively.

Since the maximum shear stress on the key is smaller than the allowable shear stress of key material with the value of 66.66 MPa, the bolts ensure the operating condition of the system.

Considering the key withstands the maximum crushing stress by the following formula [27]:

$$\sigma_{ck.max} = \frac{T \times 10^3}{L_k \times \frac{t_k}{2} \times \frac{d_{h\_I}}{2}} = 37.29 \text{ (MPa)} \quad (26)$$

where $\sigma_{ck\ max}$ is the maximum crushing stress of the square key (MPa), t_k =12 mm, and L_k = 63 mm are the width and length of the key, respectively.

Due to the crushing stress for the key material is twice its shear stress ($[\sigma_{ck}] = 2[\tau] = 133.32$ MPa) [27]. Hence, the key design ensures safety.

Designing of companion flange II connecting fly–wheel with the yoke

Figure 10 illustrates the design and dimension of companion flange II. The front flange, which has a larger outer flange diameter, is designed to follow the flywheel design. On the other hand, the back flange has a similar design to the companion flange I. The calculation and design of it are shown below.

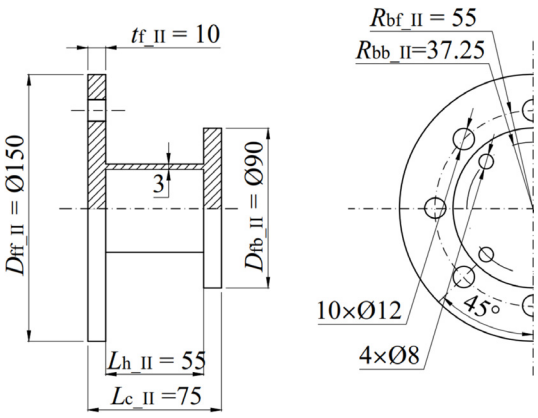

Figure 10. Drawing of companion flange II

Designing for the hub of companion flange II

According to the dimensions of the flange yoke and propeller shaft, which have been calculated and chosen above in tandem with the dimensions of the flywheel from [20]. Therefore, the outer diameter of the hub D_{h_II} is initially selected to be the same as the outer diameter of the propeller shaft D_t, which is 50 mm, and the inner diameter of the hub d_{h_II} is preliminarily selected at 44 mm. Besides, the length of hub L_{h_II} is designed to be 55 mm in order to comply with the length of the overall system. It is therefore, the polar modulus of the hub section is calculated below [26]:

$$Z_{h\_II} = \frac{\pi}{16 D_{h\_II}} \left({D_{h\_II}}^4 - {d_{h\_II}}^4 \right) = 9824.95 \text{ (mm}^3\text{)} \quad (27)$$

where Z_{h_II} is the polar modulus of the companion flange's hub connecting the flywheel with the yoke (mm^3), D_{h_II} and d_{h_II} are the outer and inner diameter of the hub with the values of 50 and 46 mm, respectively.

Hence, the following formula is used to verify the maximum shear stress of the hub [27]:

$$\tau_{h\_II} = \frac{T \times 10^3}{Z_{h\_II}} = 30.13 \text{ (MPa)} \quad (28)$$

where τ_{h_II} is the shear stress of the hub (MPa).

Since the shear stress for the hub material is less than the allowable value, the hub design is, therefore, safe.

Designing for the flange of companion flange II

The thickness of the front and back flanges (t_{f_II}) is initially chosen at 10 mm. By considering the flange at the junction of the hub, the shear stress in the flange is checked by the following formula [27]:

$$\tau_{f\_II} = \frac{T \times 10^3}{\frac{\pi {D_{h\_II}}^2}{2} \times t_{f\_II}} = 7.53 \text{ (MPa)} \quad (29)$$

where τ_{f_II} is the shear stress in the front and back flange (MPa), and t_{f_II} = 15 mm is the flange thickness.

Due to the shear stress in the flange being lower than the allowable shear stress of the material. Hence, the flange design ensures strength.

Taking into account the outer diameter of the flange yoke. Therefore, the outer diameter of the back flange D_{fb_II} is equal to the outer diameter of the flange yoke, which is 90 mm. However, the outer diameter of the front flange D_{ff_II} is followed by the dimensions of the flywheel, which is 150 mm.

Designing for bolts of companion flange II

The pitch circle radius of the flywheel bolt is 55 mm in tandem with 8 bolt holes with M12 bolt size that are already drilled. Hence, the pitch circle radius of the front flange's bolt R_{bf_II} follows the flywheel's design. Besides, the number of bolts and pitch circle radius of the back flange bolt R_{bb_II} are designed to comply with

the design of the flange yoke, the value of which is shown in Figure 10. Hence, the design of bolts for the front flange still ensures strength due to its dimensions.

5. GENERAL LAYOUT OF THE DIESEL FIREFIGHTING PUMP SYSTEM

The general layout drawing of the diesel firefighting pump system is shown in Figure 11. The propeller tube shaft (4) is assembled with two flange yokes (3) and two cross joints (6) to create a complete propeller shaft drive. DESSUN 4DSP-75 diesel engine (1) and CPHM80-32 pump (9) are attached to the base frame (8), which creates the overall length, width, and height of 2205, 1160, and 925 mm, correspondingly. The companion flange I (7) is used to connect the water pump shaft and the propeller shaft drive. On the other end, the engine flywheel is linked to the propeller shaft drive via companion flange II (2). Furthermore, the safety chuck guard (5) is applied to surround the propeller drive to ensure safety when operating. As a result, the overall system is compact in size and easy to assemble and maintain.

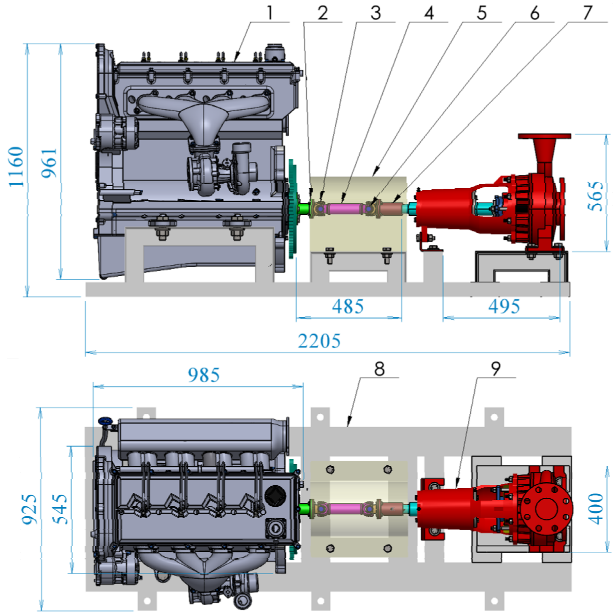

Figure 11. General layout drawing of diesel firefighting pump system

6. CONCLUSIONS

This work presents the design of a diesel engine firefighting pump system to serve high-rise buildings through the main support of AVL software. According to the current standards in Vietnam, the Kirloskar CPHM 80/32 water pump and DESSUN 4DSP-75 diesel engine were selected based on preliminary calculations to comply with the design requirements. After that, AVL software was used to simulate the speed characteristics of the selected engine by calibrating the combustion parameters and adjusting the fuel consumption. Then, a partial-load characteristic was determined to ensure the pump required input power at a rated speed of 2975 rpm. Based on the simulation results, the transmission, including the propeller drive and companion flange couplings, was designed to connect the engine and pump.

Findings show that using AVL software brings significant advantages. Instead of a practical experiment, the engine's partial load characteristics are simulated entirely on the computer, thereby reducing the cost and time. The designing process of the transmission system for the firefighting pump, therefore, also achieved the same benefits from this software.

This study can be not only considered fundamental for the calculating and designing process by quickly testing the selection of the engines and their appropriate operating mode without the need for the actual experiments but also as a role model for in-depth industry-related studies that use engines as driving sources.

ACKNOWLEDGMENT

We acknowledge Ho Chi Minh City University of Technology (HCMUT) and Vietnam National University Ho Chi Minh (VNU-HCM) for supporting this study.

The authors thank AVL LIST GmbH Hans-List-Platz 1 A - 8020 Graz, Austria, for licensed authorization to use AVL BOOST Simulation Software as part of the university partnership program.

REFERENCES

[1] Zhou, B.: Fire Situations and Prevention Measures of Residential Building. in: MATEC Web of Conferences 100, 2017, Paper 02062.

[2] Meacham, B.J., Fire safety of existing residential buildings: Building regulatory system gaps and needs, Fire Saf. J, 140, 103902, 2023.

[3] Khan, A.A., Khan, M.A., Leung, K., Huang, X., Luo, M., and Usmani, A., A review of critical fire event library for buildings and safety framework for smart firefighting, Int. J. Disaster Risk Reduct, 83, 103412, 2022.

[4] Oh, C., Kim, S., Kong, H., Development of seismic design software for firefighting pump systems. Adv. Eng. Softw, 181, 103473, 2023.

[5] Wu, S.-H.: The fire safety design of apartment buildings. MS thesis, Department of Civil Engineering, University of Canterbury, Christchurch, 2001.

[6] Bahadori, A.: Firefighting pump and water systems, in Essentials of Oil and Gas Utilities, Elsevier, Cambridge, 2016.

[7] Nolan, D.P.: Firefighting Pumping Systems at Industrial Facilities (Ed. 2nd), Elsevier, Cambridge, 2011.

[8] Heywood, B.J.: Internal combustion engine fundamentals (Ed. 2nd), McGraw-Hill Education, New York, 2018.

[9] Yüksek L, Kaleli H, Özener O, Özoğuz B. The effect and comparison of biodiesel-diesel fuel on crankcase oil, Diesel engine performance and emissions. FME Trans, 37, p. 91–7, 2009.

[10] Yu, W., Zhang, Z., Liu, B., Investigation on the Performance Enhancement and Emission Reduction of a Biodiesel Fueled Diesel Engine Based on an Improved Entire Diesel Engine Simulation Model, Processes, 9, p. 104, 2021.

[11] Zhang, Z. et al.: Effects of different mixture ratios of methanol-diesel on the performance enhancement and emission reduction for a diesel engine, Processes, 9, p. 1366, 2021.

[12] Khoa, N.X., Lim, O.: The effects of combustion duration on residual gas, effective release energy, engine power and engine emissions characteristics of the motorcycle engine, Appl. Energy, 248, pp. 54–63, 2019.

[13] Knežević, D.M., Petrović, V.S., Vorotović, G.S., Pajković, V.R., Bralović, P.D., Combustion characteristics of several types of biofuel in a diesel engine. FME Transactions, Vol. 48, pp. 319–328, 2020.

[14] An, H., Yang, W.M., Chou, S.K., Chua, K.J., Combustion and emissions characteristics of diesel engine fueled by biodiesel at partial load conditions, Appl. Energy, 99, pp. 363–371, 2012.

[15] İlhak, M.İ., Doğan, R., Akansu, S.O., Kahraman, N., Experimental study on an SI engine fueled by gasoline, ethanol and acetylene at partial loads, Fuel, 261, p. 116148, 2020.

[16] Bhandari, V.B.: *Design of machine elements*, Tata McGraw-Hill, India, 2010.

[17] Pump Performance Datasheet CPHM 80-32, Kirloskar Brothers Limited, 2015, Available from: https://www.kirloskarpumps.com/wp-content/uploads/2018/11/End-Suction-Utility-Pump-CPHM.pdf. Accessed: Sep. 09th, 2023.

[18] White, F.M.: Fluid mechanics, McGraw-Hill, New York, 2011.

[19] DSP series for fire pump model 4DSP-75. Available from: https://songhan-motor.com.vn/ upload/detail/2021/05/files/DESSUN%204DSP-75_82_5KW(2).pdf. Accessed: Sep. 09th, 2023.

[20] AVL-BOOST Theory 2022. Available from: http://www.avl.com/-/avl-boost. Accessed: Oct. 10th, 2023.

[21] Ferguson, C.R.: Internal Combustion Engines, Applied Thermosciences. John Wiley, New York, 1986.

[22] JIS G3101 General Structure Hot Rolled SS400 Steel, Material Grades, 2013, Available from: https://www.materialgrades.com/jis-g3101-general-structure-hot-rolled-ss400-steel-707.html. Accessed: Oct. 09th, 2023.

[23] Gewes: *Cardan Shaft Catalogue*, Gelenkwellenwerk Stadtilm, Thüringen, 2023.

[24] Hillier, V.A.W.: *Fundamentals of Motor Vehicle Technology*, Stanley Thornes, Cheltenham, 1990.

[25] Jon, R.M.: *Couplings and Joints: Design, selection and application*, Marcel Dekker, New York, 1999.

[26] James, M.G.: *Mechanics of Materials*, Thomson Learning, California, 2004.

[27] Khurmi, R.S., Gupta, J.K.: *A textbook of Machine Design (S.I. Units)*, Eurasia Publishing House, New Delhi, 2005.

NOMENCLATURE

D	outer diameter, mm
d	inner diameter or nominal diameter, mm
e	center of U-joint bore to end of flange yoke, mm
$F.S$	factor of safety
g	gravity acceleration, m^2/s
H	pump head, m
i	transmission ratio
L	length, mm
n	rotational speed, rpm
P	power, kW
Q	pump flow rate, m^3/s
R	pitch circle radius of bolt, mm
S	yield strength, MPa
s	size of weld joint, mm
T	torque, Nm
V	displacement volume, m^3
t	thickness, mm
w	width, mm
Z	polar modulus of section, mm^3
z	number of bolts

Greek symbols

ρ	fluid density, kg/m^3
η	efficiency
σ	allowable stress, MPa
τ	allowable shear stress, MPa

Subscripts

b	bolt
bb	back flange's bolt
bf	front flange's bolt
c	companion flange
cal	calibration
cb	crushing stress of bolt
ck	crushing stress of key
cp	cross pin
cri	critical
e	engine
exp	experiment
f	flange
fb	back flange
ff	front flange
h	hub
in	input
j	joint
k	key
out	output
p	pump
pf	propeller's flange
ps	propeller shaft
sim	simulation
t	tube
tr	transmission
y	yoke
yc	compressive yield strength
yt	tensile yield strength
weld	weld

Acronyms

BMEP	brake mean effective pressure
FMEP	friction mean effective pressure
IMEP	indicated mean effective pressure

СТУДИЈА О ПРОЈЕКТОВАЊУ СИСТЕМА ДИЗЕЛ ПУМПИ ЗА ГАШЕЊЕ ПОЖАРА ЗА СТАМБЕНУ ЗГРАДУ

Т.Д. Хонг, М.К. Фам, Ф. Гианг, Ф.Т. Труонг, Х.Х. Нгујен

Тренутно су системи дизел пумпи за гашење пожара на лицу места значајно неопходни за високе зграде. Ова студија представља процес пројектовања сис–тема дизел ватрогасних пумпи за вишеспратнице користећи АВЛ БООСТ софтвер повезан са меха–ничким прорачунима. Пумпа Кирлоскар ЦПХМ 80/32 и дизел мотор ДЕССУН 4ДСП-75 одабрани су на основу прелиминарних прорачуна како би одговарали захтевима вијетнамских стандарда за зграду од 79 метара. АВЛ БООСТ софтвер је кори–шћен за симулацију карактеристика пуног оптерећења мотора; затим се одређује карактери–стика делимичног оптерећења за адекватну пумпу која захтева улазну снагу при називној брзини од око 2975 о/мин. Пренос се састоји од погона пропелера, а прирубнице су дизајниране за повезивање мотора и пумпе. Налази показују да коришћење АВЛ БООСТ софтвера значајно помаже у одређивању карактеристика делимичног оптерећења мотора, штедећи време и трошкове. Ова студија даје основу за практична истраживања за прорачун и пројектовање механичких система пумпи за гашење пожара у високим зградама.